Article

Human Thermal Comfort and Heat Removal Efficiency for Ventilation Variants in Passenger Cars

Saboora Khatoon and Man-Hoe Kim *

Department of Mechanical Engineering, Kyungpook National University, Daegu 41566, Korea; saboorakhatoon@yahoo.com
* Correspondence: manhoe.kim@knu.ac.kr; Tel./Fax: +82-53-950-5576

Abstract: The realization of a comfortable thermal environment with low energy consumption and improved ventilation in a car has become the aim of manufacturers in recent decades. Novel ventilation concepts with more flexible cabin usage and layouts are appealing owing to their potential for improving passenger comfort and driving power. In this study, three variant ventilation concepts are investigated and their performance is compared with respect to energy efficiency and human comfort of the driver and passenger in front and a child in the rear compartment. FLUENT 16.0, a commercial three-dimensional (3D) software, are used for the simulation. A surface-to-surface radiation model is applied under transient conditions for a car parked in summer conditions with its engine in the running condition. The results for the standard Fanger's model and modified Fanger's model are analyzed, discussed, and compared for the driver, passenger, and child. The modified Fanger's model determines the thermal sensation on the basis of mean arterial pressure.

Keywords: thermal comfort; passenger car cabin; heat removal efficiency; Fanger's model; solar load

1. Introduction

Tweaking the thermal comfort inside vehicular cabins, aircrafts, and buildings, while decreasing the energy consumption is of paramount significance in indoor thermal comfort and ventilation. This is challenging in the case of an indoor environment of a vehicle cabin because of the varying position of the vehicle with time and the increasing energy consumption utilized to maintain the thermal environment with changing solar incidence angle. In addition, the indoor environment can reach a stage that causes dissatisfaction to the driver as well as the passenger in parked conditions during summer days. The increased temperature in a vehicle cabin that is not ventilated can lead to the fatality of a child that is left inside. This is because all of the air openings of the cabin are in the closed state when the vehicle is placed in the parked condition, and during this period, all of the heat is trapped by the inside air and the cabin interior materials, thus resulting in increased thermal dissatisfaction. The most important factor for realizing a pleasant thermal environment in any enclosed space is air distribution. The better the air distribution, the more homogenous temperature distribution will be achieved.

As reported by the American Society of Heating, Refrigeration and Air-Conditioning Engineering (ASHRAE), thermal comfort is specified as the condition of the mind that expresses satisfaction with thermal environment [1]. However, the sensation of thermal comfort in the human body is multifarious and in order to realize thermal comfort, the metabolic heat generated by and rejected from the human body should be equal. The size of the vehicle, incident solar radiation, number of passengers in the car, and their clothing insulation also contribute to the thermal sensation experienced by the body. However, the prime factors that contribute to human thermal comfort are physical environmental factors such as air velocity and temperature distribution.

In recent years, several researchers have numerically determined the thermal comfort for road vehicles, aircraft, and railway cabins [2]. Fišer and Jícha [3] designed the most suitable air distribution system for an aircraft cabin in order to obtain an improved quality of ventilation for the enriched thermal comfort of passengers based on the local mean age of the air using computational fluid dynamics (CFD) software. Suárez et al. [4] studied the air distribution for eight different scenarios in a railway cabin for a European environment using ANSYS-CFX, as it is challenging and costly to achieve precise results under realistic thermo-fluid conditions. The ventilation system for the thermal comfort and quality of air in public transport buses was evaluated by Zhu [5] by using a real-time continuous monitoring system. However, with the increasing awareness regarding thermal micro-environmental effects on human health in a transport vehicle, automobile car users, as well as manufacturers, are in pursuit of an improved thermal environment for car cabins with lower energy consumption.

In order to study thermal comfort in a vehicle cabin [6], the equivalent temperature model is used with varying inlet air velocities. Fojtlín [6] studied three ambient settings in a climate chamber to prevent driver fatigue in transport vehicles. He used equivalent temperature sensors as incongruous environmental parameters cause thermal stress, which negatively influences the driver's abilities. The thermal environment in transport car cabins is different from that of buildings [7]. Alahmer et al. [8] discussed various available physiological and psychological models for human thermal comfort, and Alahmer and Oma [9] performed an analysis of the relative humidity and temperature in transport vehicles using the Berekely model. The predicted mean vote (PMV), predicted percentage dissatisfaction (PPD), and equivalent temperature (EHT) models are considered as environment-based [10] models, while the dynamic thermal sensation (DTS) and Berekely comfort models are chosen for physiology-based comfort metrics.

Earlier studies on the thermal environment in car cabins [11] have investigated contaminant concentration by considering the influence of the supply and exhaust locations. Konstaninov and Wagner [12] studied four ventilation techniques for a mock-up car cabin. They divided a human manikin into 14 segments and performed a study using the finite-element code THESEUS-FE; however, the effect of solar radiation was not considered in their study. Numerical studies in the literature show that Fanger's (PMV) model is used often [13,14] for thermal comfort prediction, while some researchers [15] have considered equivalent temperature to be more appropriate. The values of the PMV from Fanger's model are not sufficient for defining the feeling of discomfort [16]; therefore, attention should be focused on this issue. Furthermore, thermal comfort models assist in identifying the cold/hot areas of the geometry that may lead to passenger discomfort and dissatisfaction, and thus, they are useful for the evaluation of the thermal requirements. In the future, the adaption and optimization of novel ventilation variants for passenger vehicles will depend on numerical flow simulations.

In addition, studies are required to appropriately estimate a child's comfort zone. On average, every year, 37 children die from heat-related deaths after being trapped inside vehicles [17]. Children have different thermal regulation characteristics from adults. The ability of a child's body to dissipate heat is very low as compared to an adult's body. Children have a higher ratio of surface area to body mass, which contributes to heat absorption in extreme environmental conditions.

Car manufacturers have improved the thermal indoor environment for drivers using various techniques. The most widely accepted standards for thermal comfort are from International Organization for Standardization (ISO), ISO 7730 standard [18] and ISO 14505 [19]. In the present study, a modified Fanger's method has been implemented to numerically predict thermal sensation. Mean blood pressure has been used as a bio-marker [20] for the evaluation of the cabin ventilation in order to improve the indoor environment for the driver and passenger, while taking the solar heat flux into consideration. An effort has also been made to evaluate the comfort zone for a child for each considered variant in the case of hyperthermia. Moreover, the heat release rate has also been calculated for predicting the energy consumption for the implemented ventilation strategy.

2. Numerical Simulation

2.1. Solver and Numerical Details of Solar Load

ANSYS FLUENT (16.0, ANSYS, Inc., Canonsburg, PA, USA) is used as a solver for the flow equations and the heat and mass transfer from and to the surfaces. The standard k–ε turbulence model is found to perform well [21] for indoor airflows, along with a high computational efficiency. The solar load is the most important factor in the consideration of the vehicle ventilation, Pawar et al. [13] presents a study of various ventilation schemes but it was recommended that the solar load be considered before implementing any ventilation strategy. The factors that can affect the solar load are the glass properties, incident solar spectrum, and solar angle of incidence. FLUENT 16.0 has an embedded solar model that uses a solar calculator to indicate the sun's direction relative to the passenger compartment, and determines the direct and diffuse solar irradiation for a specific time, date, and location. The ambient conditions for Daegu, South Korea on 21 June starting from 13:00 (local time) with a global position of latitude 35°52′ N and longitude 128°35′ E are chosen as the initial conditions with fair weather, as defined by ASHRAE. To predict the radiation exchange, a surface-to-surface radiation model that can estimate the radiation exchange in an enclosure with gray diffuse surfaces is implemented. The results obtained are validated by a comparing with the results of Sevilgen's and Kilic's [21] experimental and simulation work.

In order to calculate the direct and diffuse solar irradiation, the fair weather conditions method is implemented, which is considered as a realistic method as specified by ASHRAE. Solar irradiation of 875 W/m^2 is assigned in FLUENT, and the normal direct irradiation is calculated as

$$Edn = \frac{A}{e^{\frac{B}{\sin(\beta)}}} \tag{1}$$

where, A = apparent solar irradiation with zero air mass, B = atmospheric extinction coefficient, and β is the solar altitude above the horizontal. The conditions for the solar load are specified in Table 1.
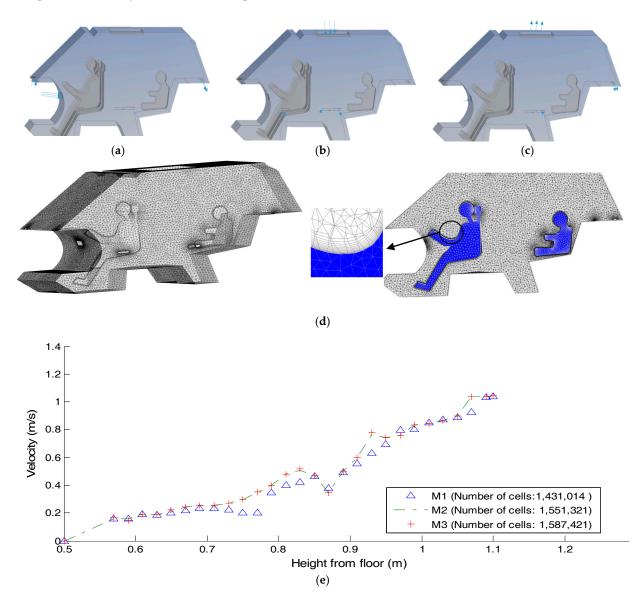
Table 1. Solar Load and Radiation Model.

Solar Load	Model
Solar radiation algorithm	Solar ray-tracing algorithm
Radiation model	S2S model with view factor
Solar irradiation	875 W/m^2

2.2. Cabin Geometry

A generic cabin car geometry with driver, passenger, and baby manikins was developed using Creo (2.0, PTC, Needham, MA, USA). All of the key design parameters were used such as the air-conditioner inlet and outlet location and windshield angle, which can affect the indoor environment for the driver and passengers as well as the ventilation. Human manikins in a sitting posture that were modeled as a driver and passenger were placed in the front compartment of the car cabin, while the rear compartment of the cabin had a baby as a passenger. The interior volume of the rear compartment, glass surface area, and the rear compartment surface area were estimated to be 2.34 m^3, 2.65 m^2, and 16.64 m^2, respectively. Three ventilation cases [13] were examined, as shown in Figure 1. In the first case, as shown in Figure 1a, air enters from the front inlets and flows out from the outlet located near the rear glass. In the second case, as shown in Figure 1b, air enters through the trickle inlet ceiling and flows out from two side slots. In the third case, as shown in Figure 1c, the fresh air enters into the cabin through porous textile bags (also known as cabin displacement ventilation inlets) and moves out from the rear and trickle inlet ceiling. However, whether these ventilation variants are suited for real cars is not discussed in the present study, as the motion of the vehicle is not taken into consideration. Unstructured mesh with triangular elements on the boundary and tetrahedral

elements for the three-dimensional (3D) region were constructed. In order to capture boundary layer accurately, fifteen prism layers were added on all of the walls. The distance of the first layer from the wall was computed to maintain the value of y+, recommended for k–ε turbulence model (ANSYS, Inc., Canonsburg, PA, USA). Moreover, element size was kept small where large gradients of flow variables were expected. Grid independence test (GID) was performed to finalize the mesh for simulations conducted for the current study. Figure 1e shows velocity profile along the height in front of driver for three mesh distributions M1, M2, and M3. It was observed that velocity profile for mesh M2 and M3 almost overlaps. Thus, M2 with less number of elements was selected for analysis based on comparable accuracy but with less computational cost.

(a)　　　　　　　　　　　　　　(b)　　　　　　　　　　　　　　(c)

(d)

(e)

Figure 1. Sketches of investigated ventilation cases with (**a**) front inlets, (**b**) trickle inlet ceiling, and (**c**) side inlets (**d**) Mesh domain (**e**) Grid independence test for velocity near driver's section.

2.3. Calculation Conditions

The simulation conditions for conduction, convection, radiation, and operating and boundary conditions were set based on experimental standards (specified by GM Korea Technical center). The analysis was performed by considering summer cooling with varying inlet positions but the same velocity value of 0.5 m/s and temperature of 13.6 °C while setting the outlet pressure as constant

atmospheric pressure. No-slip wall conditions were imposed at the wall surfaces of the windshield, seats, side and rear window, and floor of the cabin. The emissivity value of the interior surfaces was set as 0.95, while that of the glass was set as 0.88. The human manikins were considered to be wearing cotton shorts and a shirt with half-sleeves, while the rest of the body was considered uncovered set as skin. A constant heat flux value of 90.9 W/m^2, 69.93 W/m^2, and 45 W/m^2 was assigned to the driver, passenger, and baby, respectively. The cabin's convective heat transfer coefficient was set as 95 W/m^2.

The specified material properties are listed in Table 2. Fanger's model for thermal comfort is the steady state model and it was assumed in the present study that air inside the cabin is ideal and incompressible, CO_2 concentration, and volatile organic compound content that contribute to air quality are not considered, airflow inside the cabin is laminar flow due to low inlet velocities, only sensible heat dissipated by human is considered and is assumed to be evenly distributed over human body.

Table 2. Material Properties for Thermal Fluid Calculations.

Object	Material Name	Thermal Conductivity (W/m^2 K)	Density (kg/m^3)	Specific Heat (J/kg K)
Driver and passenger	Skin	0.21	1000	3770
Seat	Polyurethane foam	0.05	70	1685.60
Windshield/front & rear glass	Glass	1.171	2529.5	754
Rear & dash board	ABS plastic	2.7	996.3	1480.6

2.4. Heat Removal Efficiency

The heat removal efficiency (HRE) is calculated in order to determine the energy required to cool the car cabin. The HRE calculation requires the mean cabin temperature, and it determines the amount of energy required to maintain a certain mean temperature in the car cabin. The higher the value of the HRE, lower will be the amount of energy required for cooling the car cabin. For a fixed volume flow rate, HRE is defined as

$$\text{HRE} = 0.5 \frac{(t_{\text{exit}} - t_{\text{in}})}{(t_{\text{cabin}} - t_{\text{in}})} \tag{2}$$

2.5. Fanger's Thermal Comfort Model with Mean Blood Pressure as Biomarker

For the evaluation of thermal comfort, the PMV and PPD scales, which are used as a benchmark for calculating the human thermal comfort in vehicles, crafts, and buildings, were derived from Fanger's heat balance model. However, the authenticity of PMV/PPD model has been questioned by several studies, which has led to modification of Fanger's model, and as a result means that blood pressure was introduced as a bio marker in this model [19]. Experiment was performed for six different types of activities. The average mean arterial pressure (MAP) value as per ASHRAE standard 55, as illustrated in Figure 2.

Although, children were not involved in their experiment, Gilani et al. [20] indicates that in a thermally neutral environment, core temperature for infants and adults should be same. Core temperature is an accepted factor for metabolic rate. There are no international standards that can assist for thermal comfort evaluation of passenger vehicles.

The modified model, that depend on MAP, material properties, heat losses from outer surfaces, and heat transfer coefficient, is as follows:

$$
\begin{aligned}
mPMV = \ & \Bigg((0.303 e^{-0.036(0.1092 \times exp^{(MAP \times 0.026)})} + 0.028) \\
& \times \big\{ (0.1092 \times exp^{(MAP \times 0.0296)} - W) - 3.5 \times 10^{-3}[5733 \\
& -6.99 (0.1092 \times exp^{(MAP \times 0.0296)} - W) - p_a] \\
& -0.42 \left(\left(0.1092 \times exp^{\left(\substack{(MAP \times 0. \\ 0296)} \right)} \right) - 58.5 \right) - 1.7 \times 10^{-5} \\
& \times \left(0.1092 \times exp^{(MAP \times 0.0296)} \right) (5867 - p_a) \\
& -0.0014 \left(0.1092 \times exp^{(MAP \times 0.0296)} \right) (34 - t_a) - 3.96 \\
& \times 10^{-8} f_{cl} [(t_{cl} + 273)^4 - (t_r + 273)^4] - f_{cl} h_c (t_{cl} - t_a) \big\} \Bigg)
\end{aligned}
\tag{3}
$$

The exponential relationship between the *MAP* and activity level as follows:

$$
Activity\ Level = 0.1092 \times exp^{(MAP \cdot 0.0296)}
\tag{4}
$$

where,

W = *Effective mechanical power* (W/m^2)
p_a = Water vapor partial pressure (Pa)
t_a = *Air temperature* (°C)
I_{cl} = *Clothing insulation* (m^2 K/W)
f_{cl} = Clothing surface area factor
h_c = Convective heat transfer coefficient (W/m^2 K)
t_{cl} = Clothing surface temperature (°C)

The convective heat transfer coefficient (h_c) and the clothing surface temperature (t_{cl}), as defined in Equations (6) and (7), are solved using iterative method.

$$
f_{cl} = \begin{cases} 1.00 + 1290 \times I_{cl}\ for\ I_{cl} \leq 0.078\ \text{m}^2\text{K/W} \\ 1.05 + 0.645 \times I_{cl}\ for\ I_{cl} > 0.078\ \text{m}^2\text{K/W} \end{cases}
\tag{5}
$$

$$
h_c = \begin{cases} 2.38 |t_{cl} - t_a|^{0.25}\ for\ 2.38 |t_{cl} - t_a|^{0.25} > 12.1\ \sqrt{v_a} \\ 12.1 \sqrt{v_a}\ for\ 2.38 |t_{cl} - t_a|^{0.25} < 12.1\ \sqrt{v_a} \end{cases}
\tag{6}
$$

$$
t_{cl} = 35.7 - 0.028(M - W) - I_{cl} \{ 3.96 \times 10^{-8} \times f_{cl} [(t_{cl} + 273)^4 - (t_r + 273)^4] + f_{cl} \times h_c \times (t_{cl} - t_a) \}
\tag{7}
$$

The mean radiant temperature (t_r) is defined as the uniform temperature of the walls in an area in which someone would trade an indistinguishable measure of warmth by radiation as in the real condition and is calculated as;
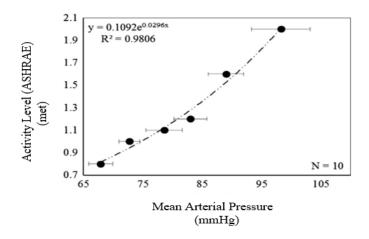
$$
t_r = \sqrt[4]{\sum_n F_{p-i} (t_i + 273)^4} - 273
\tag{8}
$$

The term (t_i) in Equation (8) is the surface temperature of the immediate surface *i*. Based on known mPMV value, the corresponding mean PPD can be calculated. The PPD model is used to predict the number of people who are most likely to feel uncomfortable in a specified environment, as shown in Figure 3.

The mPPD is evaluated as;

$$
mPPD = 100 - 95 exp \left(-0.03353 mPMV^4 - 0.2179 mPMV^2 \right)
\tag{9}
$$

To specify comfort sensation, an index that takes the values of 3 = hot, 2 = warm, 1 = slightly warm, 0 = comfortable/neutral, −1 = slightly cool, −2 = cool, and −3 = cold is used. The estimated PMV and mPMV index will be used to predict the thermal response of the driver, passenger, and baby, according to ASHRAE thermal sensation scale. Generally, PMV index is used to predict the mean response of the thermal vote of an extensive gathering of individuals that were exposed to similar environmental conditions. Be that as it may, input parameters are changed in modified Fanger model with the goal that it might give better outcome for inhomogeneous environment like passenger car cabin.

Figure 2. Mean arterial pressure (MAP) and American Society of Heating, Refrigeration and Air-Conditioning Engineering (ASHRAE) metabolic activity.
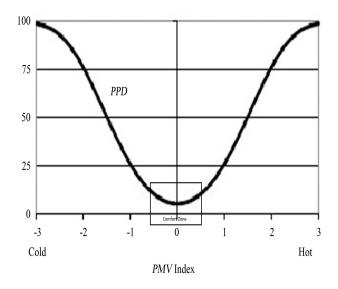

Figure 3. Predicted percentage dissatisfaction (PPD) as a function of predicted mean vote (PMV).

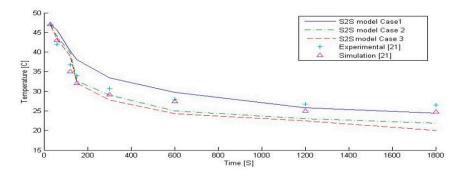## 3. Results and Discussion

3.1. Computed Temperature and Velocity Flow Fields

The objective of this study was to investigate the novel ventilation schemes with respect to the spectral characteristics of the opto-energy transport in a car cabin and, more specifically, a rear compartment under solar radiation. The decrease in interior temperature is plotted against time in Figure 4. The temperature profile and velocity vectors formed under each ventilation scheme are shown in Figure 5 on a vertical plane at a distance of "+x" equals 0.6 m. Under the conventional inlet positions, i.e., front inlets only, the flow from the inlets was blocked by the driver and passenger,

thus resulting in large recirculation flows in front area of the car cabin. This air recirculation, as shown in Figure 5b, was effective in lowering the temperature of the cabin from the high temperature caused by solar radiation, as shown in Figure 5a. This cooled air then moves through the space between the two front seats. The recirculation pattern of the air exhibits a velocity magnitude of 0.12 m/s near the child manikin that is placed in the rear compartment of the cabin.

In case 2, wherein the air enters from the roof and flows out from the side outlets, as shown in Figure 5d, the air circulation pattern in the front and rear compartment is almost the same. The lowering of temperature in the front compartment takes more time than the rear compartment, as shown in Figure 5c, owing to the solar radiation. While, in case 3, as demonstrated in Figure 5e, wherein the air flows from the top as well as the front side inlets, the turbulence in the air flow is greater than in the other cases. However, the temperature decreased much faster in this case than in the earlier cases.

The total simulation time was 30 min as the majority of car trips are shorter than 18 km, which lasts only up to 30 min [22]. In case of transient simulation times, the step size is critical, and the time step size at the beginning of the transient simulation affects the end results and is crucial for obtaining satisfactory as well as precise simulation results. For the current simulation, the initial time step was set as 0.001 s for the first 5 min of cooling and then to 1 s for the rest of the numerical simulation.

Figure 4. Cabin interior air temperature comparison for each considered case and previous results (adapted from [21]) for the cooling process.
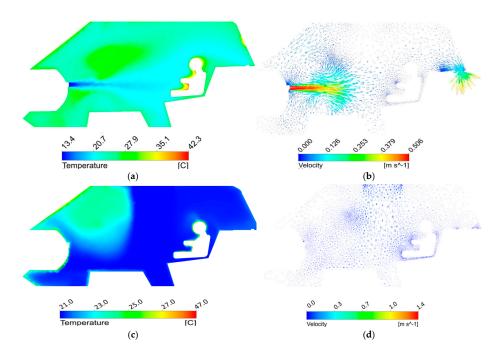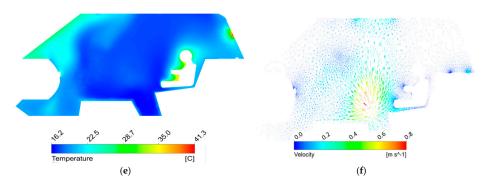

Figure 5. *Cont.*

Figure 5. Predicted temperature and velocity fields for all of the considered variants. Case 1 (**a**) Temperature profile and (**b**) Velocity contours. Case 2 (**c**) Temperature profile and (**d**) Velocity contours. Case 3 (**e**) Temperature profile and (**f**) Velocity contours.

3.2. Heat Removal Efficiency for Novel Schemes

In Figure 5a,c,e, the temperature distribution for each case is presented. High-temperature values were obtained for case 1. The mean cabin temperature predicted for cases 1, 2, and 3, are 24.42 °C, 21.85 °C, and 19.95 °C, respectively. Based on these known values of temperature, the HRE can be calculated for each case. The HRE, as defined in Equation (2), aids in determining the amount of energy required to maintain a certain value of temperature inside the car cabin. For a fixed volume flow rate, HRE is in direct proportion to the amount of thermal energy that the air has absorbed in the cabin. An HRE value of 0.5 is considered to be the best possible value for ventilation [13]. If the heat source is near the exit, the HRE value can be as great as 0.5. The higher the value of HRE, the lower is the amount of energy required to cool the passenger cabin. The computed HRE values for each case are presented in Table 3, which shows that case 1 has a higher heat flux from the occupants in the cabin followed by the other techniques.
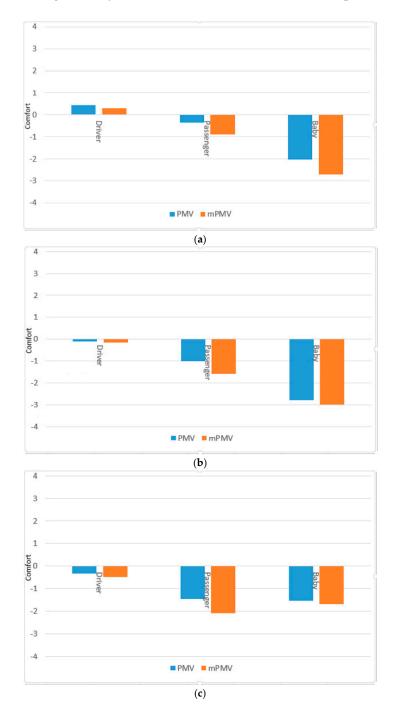
Table 3. Estimated Mean Cabin Temperature and heat removal efficiency (HRE) Value for All Considered Cases.

Case No.	Cabin Mean Temperature	Heat Removal Efficiency
Case 1	24.42 °C	0.51
Case 2	21.85 °C	0.48
Case 3	19.95 °C	046

3.3. Comfort Predictions

Thermal comfort, in particular, is not considered as a rational experience, but as an emotional experience. To date, for the evaluation of thermal comfort, the designed scale is "comfortable" and "uncomfortable" or "pleasant" and "unpleasant". The CFD results are conveyed to Fanger's model to evaluate the thermal comfort for any specified environment. Fanger's model is a steady-state and homogenous model that relies on PMV. The predicted thermal vote value for the whole body is then plotted according to ASHRAE thermal sensation scale. To estimate the PMV and mPMV values, the temperature, mean radiant temperature, and velocity of the air are obtained from simulation results. The metabolic activities [23,24] of 1.4 met, 1 met, and 0.7 met [25] are assigned to the driver, passenger, and baby, respectively, which correspond to 80 W/m^2, 58.2 W/m^2, and 45 W/m^2 [26], respectively, and the corresponding MAP value is estimated using Equation (4). The external work value is specified as zero. Although, relative humidity does not have a strong influence on the thermal comfort, people usually feel comfortable at a range of relative humidity values provided that the temperature is comfortable. A constant humidity value of 65% is assumed. The calculated results are then compared with those of the modified Fanger's model, which is labelled as mPMV in Figure 6.

As can be observed in Figure 6, the calculated values from each model for all of the considered variants for the driver are within the comfort zone. The passenger sitting next to the driver is in the comfort zone for cases 1 and 2, while they are slightly uncomfortable for case 3 as per the improved Fanger's model. However, the prediction for the infant child at the rear compartment is in an uncomfortable zone in case of each model. The minimum deviation between the estimated values obtained from each model is approximately 20%. It is also observed from the calculated values that the spectral solar radiation significantly affects the thermal comfort of the occupants.

(a)

(b)

(c)

Figure 6. Predicted thermal comfort for the three considered ventilation cases after 30 min of cooling. (**a**) Case 1. (**b**) Case 2. (**c**) Case 3.

4. Conclusions

In this study, the combined heat transfer characteristics for solar radiation in a generic car model with novel ventilation schemes are numerically evaluated. The modified Fanger's model is applied, keeping in mind the spectral radiation effects, and each ventilation scheme is investigated to obtain the following conclusions:

1. The numerical predictions discussed above are based on the standard k–ε model, as well as surface-to-surface radiation model for transient conditions. The results of the numerical simulations showed that human thermal comfort in the passenger car cabin and energy efficiency is influenced by the applied ventilation variant.
2. Modified Fanger's model, which is developed by the estimation approach of activity level stated as per ASHRAE standard 55 provides results with 20% improvement for thermal sensation. Thermal comfort is predicted for each ventilation scheme for 30 min of cooling based on the length of majority of car trips.
3. An effort has been made to numerically predict the comfort zone for a child in the rear compartment of the cabin. The estimated mean vote values from the standard Fanger's and modified Fanger's models for a child lie in a slightly uncomfortable zone; furthermore, a full-scale review is required for deriving a child's comfort zone, as well as the possible reasons that can cause fatalities in infants.
4. The alternative ventilation strategies were evaluated for HRE as well as the thermal comfort. For case 3, the airflow was more homogenous, and the predicted values for a child were within the comfort zone.

Author Contributions: Saboora Khatoon performed the numerical analysis and drafted the manuscript. Man-Hoe Kim supervised the research and edited the manuscript. The authors have read and approved the manuscript.

Conflicts of Interest: The authors declare no conflict of interest.

Nomenclature

A	Apparent solar irradiation (W/m^2)
B	Atmospheric extinction coefficient (m)
β	Solar altitude
Edn	Normal direct irradiation
M	Metabolic rate (W/m^2)
PMV	Predicted mean vote
PPD	Predicted percentage dissatisfaction
HRE	Heat removal efficiency
MAP	Mean arterial pressure
S2S	Surface to surface
GID	Grid independent test
W	Effective mechanical power (W/m^2)
p_a	Water vapor partial pressure (Pa)
t_a	Air temperature (°C)
I_{cl}	Clothing insulation (m^2 K/W)
t_r	Mean radiant temperature (°C)
t_i	Surface temperature of immediate surface i
$F_{p\text{-}i}$	View factor between the person and surface i
h_c	Convective heat transfer coefficient (W/m^2 K)

f_{cl}	Clothing surface area factor
t_{cl}	Clothing surface temperature (°C)
v_a	Relative air velocity (m/s)
t_{in}	Inlet temperature (°C)
t_{cabin}	Mean temperature of cabin (°C)
t_{exit}	Outlet temperature (°C)

References

1. American Society of Heating, Refrigerating and Air Conditioning Engineers (ASHRAE). *ASHRAE Standard 55-2013 Thermal Environmental Conditions for Human Occupancy*; Ashrae: New York, NY, USA, 2013.
2. Aliahmadipour, M.; Abdolzadeh, M.; Lari, K. Air flow simulation of HVAC system in compartment of a passenger coach. *Appl. Therm. Eng.* **2017**, *123*, 973–990. [CrossRef]
3. Fišer, J.; Jícha, M. Impact of air distribution system on quality of ventilation in small aircraft cabin. *Build. Environ.* **2013**, *69*, 171–182. [CrossRef]
4. Suárez, C.; Iranzo, A.; Salva, J.; Tapia, E.; Barea, G.; Guerra, J. Parametric Investigation Using Computational Fluid Dynamics of the HVAC Air Distribution in a Railway Vehicle for Representative Weather and Operating Conditions. *Energies* **2017**, *10*, 1074. [CrossRef]
5. Zhu, S.; Demokritou, P.; Spengler, J. Experimental and numerical investigation of micro-environmental conditions in public transportation buses. *Build. Environ.* **2010**, *45*, 2077–2088. [CrossRef]
6. Fojtlín, M.; Fišer, J.; Pokorný, J.; Povalač, A.; Urbanec, T.; Jícha, M. An innovative HVAC control system: Implementation and testing in a vehicular cabin. *J. Therm. Biol.* **2017**. [CrossRef]
7. Shin, Y.; Im, G.; Yu, K.; Cho, H. Experimental study on the change in driver's physiological signals in automobile HVAC system under Full load condition. *Appl. Therm. Eng.* **2017**, *112*, 1213–1222. [CrossRef]
8. Alahmer, A.; Mayyas, A.; Mayyas, A.A.; Omar, M.A.; Shan, D. Vehicular thermal comfort models; A comprehensive review. *Appl. Therm. Eng.* **2011**, *31*, 995–1002. [CrossRef]
9. Alahmer, A.; Omar, M. Vehicular Cabins' Thermal Comfort Zones—Fanger and Berkley Modeling. *Veh. Eng.* **2013**, *1*, 19–32.
10. Hepokoski, M.; Curran, A.; Schwenn, T. A Comparison of Physiology-Based Metrics to Environment-Based Metrics for Evaluating Thermal Comfort. *SAE Tech. Pap.* **2013**. [CrossRef]
11. Wan, J.W.; van der Kooi, J. Influence of the position of supply and exhaust openings on comfort in a passenger vehicle. *Int. J. Veh. Des.* **1991**, *12*, 588–597.
12. Feldmann, D.; Wagner, C. *New Results in Numerical and Experimental Fluid Mechanics VIII*; Springer: Berlin, Germany, 2013; Volume 121.
13. Pawar, S.; Gade, U.R.; Dixit, A.; Tadigadapa, S.B.; Jaybhay, S. Evaluation of Cabin Comfort in Air Conditioned Buses Using CFD. *SAE Tech. Pap.* **2014**. [CrossRef]
14. Vartires, A.; Dogeanu, A.; Danca, P. The human thermal comfort evaluation inside the passenger compartment. In Proceedings of the International Multidisciplinary Scientific GeoConferences (SGEM), Albena, Bulgaria, 18–24 June 2015; Volume 1, pp. 1113–1120.
15. Foda, E.; Sirén, K. Evaluating the thermal comfort performance of heating systems using a thermal manikin with human thermoregulatory control. *Indoor Built Environ.* **2016**, *25*, 191–202. [CrossRef]
16. Simion, M.; Socaciu, L.; Unguresan, P. Factors which Influence the Thermal Comfort Inside of Vehicles. *Energy Procedia* **2016**, *85*, 472–480. [CrossRef]
17. Scutti, S. Hot Car Deaths Reach Record Numbers in July. CNN 3 August 2017. Available online: http://edition.cnn.com/2017/08/01/health/hot-car-deaths/index.html (accessed on 25 October 2017).
18. *ISO 7730:2005 Ergonomics of the Thermal Environment Analytical Determination and Interpretation of Thermal Comfort Using Calculation of the PMV and PPD Indices and Local Thermal Comfort Criteria*; International Organization for Standardization: Vernier, Switzerland, 2005.
19. *ISO 14505-2:2006 Ergonomics of the Thermal Environment-Evaluation of Thermal Environments in Vehicles-Part 2: Determination of Equivalent Temperature*; International Organization for Standardization: Vernier, Switzerland, 2006.
20. Gilani, S.I.U.H.; Khan, M.H.; Ali, M. Revisiting Fanger's thermal comfort model using mean blood pressure as a bio-marker: An experimental investigation. *Appl. Therm. Eng.* **2016**, *109*, 35–43. [CrossRef]

21. Sevilgen, G.; Kilic, M. Investigation of transient cooling of an automobile cabin with a virtual manikin under solar radiation. *Therm. Sci.* **2013**, *17*, 397–406. [CrossRef]

22. Fojtlín, M.; Pokorný, J.; Fišer, J.; Toma, R.; Tuhovþák, J. Impact of measurable physical phenomena on contact thermal comfort. *EPJ Web Conf.* **2017**, *143*. [CrossRef]

23. Garcia-Souto, M.D.P.; Dabnichki, P. Core and local skin temperature: 3–24 months old toddlers and comparison to adults. *Build. Environ.* **2016**, *104*, 286–295. [CrossRef]

24. Baskovic, U.Z.; Lorenz, M.; Butala, V. Adiabatic flow simulation in an air-conditioned vehicle passenger compartment. *Int. J. Simul. Model.* **2014**, *13*, 42–53. [CrossRef]

25. Kliegman, R.M.; Stanton, B.M.D.; Geme, J.S.; Schor, N.F. *Nelson Textbook of Pediatrics*; Elsevier: Phialdelphia, PA, USA, 2015; p. 3408.

26. Han, T.; Huang, L. A model for relating a thermal comfort scale to EHT comfort INDEX. *SAE Tech. Pap.* **2004**. [CrossRef]